JOURNAL OF CATALYSIS **130**, 556–568 (1991)

Hydrogenolysis of Methylcyclopropane on Oxygen-Modified Mo(111): The Appearance of Acid Sites

M. S. TOUVELLE AND P. C. STAIR

Department of Chemistry, Northwestern University, Evanston, Illinois 60208

Received October 9, 1990; revised April 3, 1991

Catalytic evidence for oxide formation on the Mo(111) surface has been obtained using methylcyclopropane (MCP) hydrogenolysis as a probe reaction. These results have been correlated with physical measurements made on the O/Mo system. Oxide formation on Mo has been studied previously by monitoring surface polarizability using XPS of physisorbed xenon. The results from this study concluded that oxide begins to form at 1×10^{15} atoms/cm^2 and is essentially completely formed by 1.4×10^{15} atoms/cm^2. Catalytic hydrogenolysis of methylcyclopropane to i-C_4H_{10}, n-C_4H_{10}, C_3H_8, C_2H_6, and CH_4 has been investigated over initially clean Mo(111) surfaces, surfaces chemically modified by oxygen coverages of 0–2 $\times 10^{15}$ atoms/cm^2 and MoO_2. Catalyst preparation was performed in UHV with surface characterization by LEED and Auger. Hydrogenolysis at 1 atm pressure (5 Torr MCP, 755 Torr H_2) was monitored by gas chromatography. MCP can undergo single hydrogenolysis by either a metallic or a Lewis/Brønsted acid mechanism depending upon the chemical state of Mo. The metallic function of the catalyst dominated at oxygen coverages of $<1 \times 10^{15}$ atoms/cm^2 to form i-C_4H_{10}. In addition, the product distribution (60% i-C_4H_{10}, 11.5% n-C_4H_{10}, 14% C_3H_8, 14% CH_4, 0.5% C_2H_6) remained constant up to an oxygen coverage of 1×10^{15} atoms/cm^2. At oxygen coverages $>1 \times 10^{15}$ atoms/cm^2, the i-C_4H_{10} rate fell to zero. At a coverage of 1.5×10^{15} atoms/cm^2, the acidic function of the catalyst began to dominate, and the n-C_4H_{10} rate increased by a factor of five. At this coverage n-C_4H_{10} was the sole single hydrogenolysis product. No double hydrogenolysis occurred on surfaces with high O coverage. Thus the catalytic results, which indicated Lewis/Brønsted acid sites were formed at an O coverage of 1.5×10^{15} atoms/cm^2, agreed well with the XPS measurements which have shown that oxide was completely formed at 1.4×10^{15} atoms/cm^2. © 1991 Academic Press, Inc.

INTRODUCTION

The reactions of H_2 with various alkylcyclopropanes

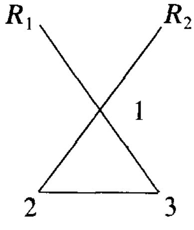

($R_1 = CH_3, C_2H_5$, etc., $R_2 = H, CH_3, C_2H_5$, etc.) have been studied previously over numerous transition metal and metal oxide surfaces. The presence of the alkyl group as well as the acidity of the catalyst is found to have an effect on which ring C–C bond will be preferentially activated. In general, the C_2–C_3 bond is preferentially broken on metal surfaces. The explanation generally given for the selectivity on metal catalysts is that the electron-releasing alkyl group(s) exerts an inductive effect on the cyclopropane ring so as to increase the electron density in the C–C bonds adjacent to the point of substitution (*1–3*). The C_2–C_3 bond is the weakest bond; therefore, it is the one that is broken. This effect has been observed on many different metal catalysts including Pd (*4–6*), Pt (*4–6*), Ni (*4–6*), Rh (*5*), Co (*5*), and Fe (*5*) films as well as Pt/Al_2O_3 (*4, 5, 7, 8*)-, Pt/pumice (*3, 4, 7*)-, Ir/Al_2O_3 (*5*)-, Ni/kieselguhr (*7, 9*)-, Pt/SiO_2 (*10–12*)-, and Rh/SiO_2 (*13*)-supported catalysts. The only exceptions to this trend have been observed

0021-9517/91 $3.00

on W (*5*, *6*) and Au (*5*) films, Ir(111) and (110)1 × 2 single-crystal surfaces (*14*), and $Mo(0)/Al_2O_3$ (*15*, *16*)-supported catalysts.

Alkylcyclopropanes react by a different mechanism over acidic catalysts (*17*). Over catalysts with a Brønsted acid function, carbenium ions are formed during the ring-opening process. Cleavage of the bond between the ring carbon attached to the alkyl group and an adjacent carbon (C_1–C_2 or C_1–C_3) is preferred because the carbenium ion formed is the most stable. If the C_2–C_3 bond is cleaved, a primary carbenium is formed which is unstable. However, if the C_1–C_2 bond in a singly substituted cyclopropane is cleaved, a more stable secondary carbenium ion is formed. Likewise, a tertiary carbenium ion is formed from the C_1–C_2 cleavage in a 1,1-disubstituted cyclopropane.

Lewis acidity has also been proposed to account for preferential cleavage of the C_1–C_2 or C_1–C_3 bond. Electrophilic attack by Cu cations (Lewis acid) has been suggested to be responsible for the regioselectivity in the hydrogenative ring opening of alkylcyclopropanes over Cu/SiO_2 catalysts (*18*, *19*). Thus, whether a catalyst has Lewis or Brønsted acidity, one can use the change in selectivity of bond cleavage, C_2–C_3 versus C_1–C_2 as a probe for acid site formation.

In this paper we report on an experimental investigation of the hydrogenolysis of methylcyclopropane (MCP) over an initially clean Mo(111) surface, surfaces modified with oxygen coverages between 0 and 2×10^{15} atoms/cm^2, and MoO_2. Two single-hydrogenolysis products are obtained from the reaction of MCP and H_2. Isobutane is the major product formed on metallic sites, whereas, *n*-butane is the major product formed on Lewis/Brønsted acid sites. Double hydrogenolysis can also occur, and on Mo catalysts at 373 K (the catalyst temperature used in this study), equal amounts of methane and propane are formed along with a small amount of ethane (*15*, *16*). Complete fragmentation to methane has not been observed on Mo catalysts at 373 K. Changes in isobutane and *n*-butane selectivities can be used as catalytic probes for oxide formation. Double hydrogenolysis product distributions give additional information on possible reaction intermediates.

We attempt to correlate the catalytic data presented here to previous physical measurements made on the O/Mo system (*20*, *21*). More specifically, we show that the onset of Lewis/Brønsted acid catalysis on these surfaces is coincident with oxide formation on molybdenum. The metal-to-oxide transition on the Mo(100) surface has been studied previously by monitoring surface polarizability using X-ray photoelectron spectroscopy (XPS) measurements of physisorbed xenon (*20*, *21*). The surface polarizability was found to decrease slowly between 0 and 1×10^{15} O atoms/cm^2 followed by an abrupt decrease in polarizability at higher coverages which signaled an abrupt metal-to-oxide transition. Below 1×10^{15} atoms/cm^2, oxygen was solely in a chemisorbed phase. There was evidence of surface heterogeneity for oxygen coverages between 1 and 1.4×10^{15} atoms/cm^2. It was suggested that an island structure consisting of patches of oxide and chemisorbed oxygen coexist in this coverage range. The polarizability of a Mo(100) surface with an O coverage of 1.4×10^{15} atoms/cm^2 was approximately the same as that of MoO_2. Thus a Mo(100) surface is completely covered with oxide at a coverage of 1.4×10^{15} atoms/cm^2.

In another study (*22*), the surface Mo oxidation states for a Mo(100) surface modified with 0–1.4×10^{15} O atoms/cm^2 were measured using XPS. The shift in binding energy of the Mo($3d_{5/2}$) peak with increasing O coverage was monitored. The surface with 1.4×10^{15} atoms/cm^2 was assigned an oxidation state of +4, and the oxidation states for the remainder of the modified surfaces were assigned proportional to the binding energy shift for that surface. Two regimes were evident in the Mo XPS experiments which was also what was found in the Xe XPS work. For oxygen coverages $<1 \times 10^{15}$ atoms/cm^2, the surface Mo oxidation state remained constant at ca. +1. Between 1 and 1.4×10^{15} atoms/cm^2, there was a rapid change in the Mo oxidation state to +4.

In addition, the surface oxide has been shown to have the same chemical adsorption selectivity for various molecules as MoO_2 (*23*). Below 1×10^{15} O atoms/cm^2, the surface was extremely reactive, causing dissociative adsorption at room temperature. The surface reactivity decreased dramatically between 1 and 1.5×10^{15} atoms/cm^2 with nitrogen-containing bases (eg., NH_3, CH_3NH_2, pyridine) being adsorbed strongly and π-electron donors being only weakly adsorbed. It was concluded that the chemisorption of these molecules is of a Lewis acid/base type, and the acid sites are localized, probably being associated with electron deficient Mo cations. These three studies have shown convincingly that oxygen is in a chemisorbed phase below 1×10^{15} atoms/cm^2, oxide patches form between 1 and 1.5×10^{15} atoms/cm^2 and that surface oxide is completely formed by 1.5×10^{15} atoms/cm^2.

One might question whether it is correct to assume that MoO_2 forms at the same oxygen coverage on the Mo(111) surface as it does on the Mo(100) surface. Although different ordered overlayer structures have been observed on the two surfaces at low oxygen coverage ($<1 \times 10^{15}$ atoms/cm^2), it appears that the conditions required to produce oxide on the two surfaces are very similar. Kennett and Lee used reflectance high-energy electron diffraction to show that the exposure needed to produce oriented oxide on Mo(111), (100), and (110) surfaces at a given temperature was similar (*24, 25*). Zhang *et al.* (*26*) used AES and LEED to probe the high-temperature oxidation of the Mo(100) and (111) surfaces. Again, the results show that very similar conditions produced oxide on both surfaces. Although a detailed investigation of oxide formation on the Mo(111) surface has not been undertaken, it appears valid to apply the results from the (100) surface to the (111) surface.

METHODS

Experiments were performed in a UHV chamber (base pressure of 2×10^{-10} Torr) equipped with two ion pumps and a titanium sublimator. The chamber is also equipped with a quadrupole mass spectrometer, LEED optics, 0- to 5-kV ion gun, microcapillary array doser, cylindrical mirror analyzer for Auger electron spectroscopy, and a 0.1-liter volume high-pressure reactor. Schematic diagrams of the UHV chamber and high-pressure reactor have been presented previously (*27*).

The Mo single crystal was oriented to within ±1° of the (111) plane. The crystal was polished with successively finer grades of SiC, diamond paste, and alumina (Buehler) down to 0.03 μm and then bulk cleaned of carbon and sulfur by heating in 5×10^{-7} Torr O_2 at ca. 1500 K for 48 h. The sample was mounted edge on to a precision manipulator by spotwelding to stainless-steel support rods. The sample could be heated resistively to 1300–1400 K through the supports. The temperature was monitored by a chromel–alumel thermocouple spotwelded to the side of the crystal away from the stainless-steel support rods.

The oxygen-modified Mo surfaces were prepared by first cleaning the surface with Ar^+ sputtering followed by annealing to 1300–1400 K to restore surface order. The crystal was then exposed to Matheson research grade O_2 through a microcapillary array doser. To obtain oxygen coverages below 1.7×10^{15} atoms/cm^2, the dose was performed with the crystal at room temperature, followed by a short anneal at 650 K. The clean Mo(111) surface gave a $p(1 \times 1)$ LEED pattern with quasihexagonal symmetry. No ordered O overlayer structures could be observed from room-temperature adsorption. The substrate spots decreased in intensity with a concomitant increase in background intensity during oxygen adsorption. The samples were annealed at 650 K because the Mo(111) surface facets with moderate oxygen coverages and annealing temperatures >1000 K (*25, 26, 28, 29*). There was no LEED evidence for faceting under the conditions employed here. No LEED patterns were observed for surfaces with oxygen coverages >1.3 × 10^{15} atoms/cm^2 at energies <200 eV. To obtain O coverages above 1.7 × 10^{15} atoms/cm^2 it was necessary to perform the dose with the crystal at 650 K. MoO_2 was formed by heating the crystal to 925 K and exposing it to ca. 25,000 L O_2. This procedure was similar to that followed in Ref. (*30*) to produce surface MoO_2. The O(503 eV)/Mo(221 eV) Auger peak-to-peak ratio obtained in this experiment was in close agreement with that obtained in Ref. (*30*). Raman spectroscopy results also indicate that MoO_2 has formed under these conditions (*31*). No LEED pattern was observed after the surface oxide preparation. A LEED pattern corresponding to a MoO_2(100) lattice has been reported (*26*); however, the conditions of preparation were different than those used in this study.

Oxygen coverages were determined by Auger using the O(503 eV)/Mo(221 eV) peak-to-peak ratio and a sensitivity factor obtained by signal calibration against the saturated β-CO adsorption state on Mo(100) (*32*). Two corrections had to be made to the sensitivity factor to obtain accurate O coverages for the (111) surface. The first correction took into account the different unit cell areas for the (111) and (100) surfaces which are 17.07 and 9.86 $Å^2$, respectively. The second correction involved a small difference in the calculated Mo(221 eV) Auger peak intensity for the two surfaces. Oxygen coverages reported here were the average of three measurements taken at three different spots on the crystal prior to reaction. Three measurements were also taken after the reaction to check for carbon deposition and/or oxide reduction. The coverage determination by Auger is accurate to ±1 × 10^{14} atoms/cm^2.

The MCP used here was 98% purity from Columbia Organic Chemical Co. The hydrogen was Matheson UHP. Since the main objective of this study was to evaluate the activity and selectivity of the single-crystal catalyst as a function of O coverage, extreme care was taken to minimize surface contamination by oxygen-containing species such as H_2O and O_2. Manganese oxide and silica traps were used for removal of trace amounts of H_2O and O_2. In addition, the MCP was degassed at 80 K and the H_2 was passed through a liquid N_2 cooled trap. These procedures were sufficient to eliminate surface contamination. Typical hydrocarbon impurities in the MCP, as determined by GC, were 0.005% CH_4, 0.02% C_2H_6, 0.0035% C_3H_8, 0.074% C_3H_6, 0.0034% i-C_4H_{10}, 0.339% n-C_4H_{10}, and 0.622% 1-C_4H_8. Corrections were made for the initial impurity levels in all turnover frequency (TOF) and product distribution calculations.

Reaction conditions for the experiments reported here were 5 Torr MCP, 750 Torr H_2, and a crystal temperature of 373 K. The stainless-steel reactor and back side of the crystal were passivated using H_2S. The detailed procedures are described elsewhere (*27*). Periodic checks were made to ensure that the reactor remained inactive by inserting a stainless-steel blank in place of the Mo crystal. The reactor contribution to isobutane and double hydrogenolysis product formation was negligible (<0.1%). The background contribution to the n-butane rate from the reactor amounted to ca. 20% of the production at oxygen coverages <1.5 × 10^{15} atoms/cm^2 and to ca. 4% of the production at oxygen coverages >1.5 × 10^{15} atoms/cm^2. The reactor contribution has been subtracted from all n-butane data presented here.

The reactor used was of the batch circulation type. Constant volume GC samples were periodically removed over approxi-

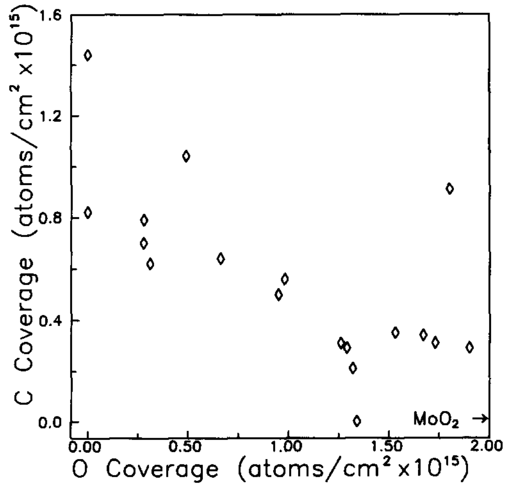

FIG. 1. Carbon coverage following reaction as a function of oxygen precoverage.

mately a 2-h reaction period. The reactant loss due to sampling was taken into account when evaluating chromatographic peak heights. A more detailed description of the reaction procedure is given in Ref. (*27*).

RESULTS

Methylcyclopropane hydrogenolysis was observed at a temperature of 373 K on the initially clean Mo(111) surface, on surfaces modified with oxygen coverages between 0 and 2 × 10^{15} atoms/cm^2, and on MoO_2. The conversion of MCP over a 2-h period at 373 K was 5–15%. Products detected were isobutane, *n*-butane, propane, ethane, and methane. 1-Butene, propene, *cis*-2-butene, *trans*-2-butene, pentane, and 1-butyne also were detected during two runs over surfaces with high oxygen precoverage. Surface reduction under the reaction conditions employed here was not observed. Oxygen coverages before and after a reaction were identical within ±1 × 10^{14} O atoms/cm^2. Carbon deposition was detected by Auger following the reaction. In general, the amount of carbon deposited decreased with increasing oxygen precoverage as shown in Fig. 1.

Figure 2 shows isobutane and *n*-butane accumulation curves for two surfaces; one with low oxygen precoverage and one with high oxygen precoverage. Double hydrogenolysis product accumulation curves are very similar to those shown in Fig. 2 and are not presented here. Rates of reaction were computed from plots of product accumulation as a function of time. Since no deactivation was observed for any of the product accumulation curves, rates were computed from a linear least-squares fit to the data. All top-layer Mo atoms (n_s = 5.85 × 10^{14} Mo atoms/cm^2) were counted in the computation of TOFs for the initially clean Mo(111) surface as well as the oxygen-modified sur-

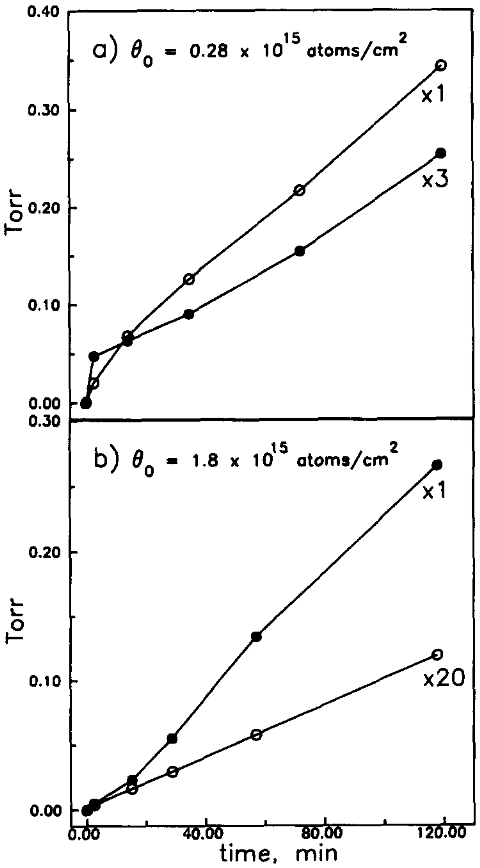

FIG. 2. Isobutane and *n*-butane accumulation curves on surfaces with low and high oxygen precoverage. (a) θ_0 = 0.28 × 10^{15} atoms/cm^2, (b) θ_0 = 1.8 × 10^{15} atoms/cm^2; (○) isobutane, (●) *n*-butane.

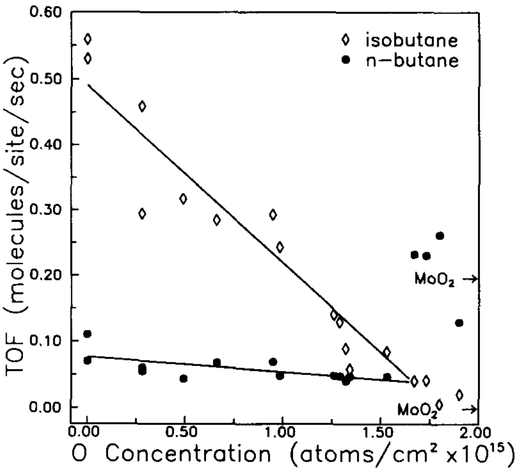

FIG. 3. Turnover frequencies for isobutane and *n*-butane formation as a function of oxygen precoverage.

faces. This procedure only gives accurate TOFs for all surfaces if the active site density is constant for all surfaces investigated. This assumption is probably not correct; however, there is no meaningful way to measure the active site density on each surface. In any case, even if the TOF values are only estimates, meaningful comparisons between surfaces can be made and trends may be interpreted.

The catalytic results differ significantly depending upon oxygen precoverage. Therefore, the results are divided into two sections; one describing results on surfaces with less than 1×10^{15} O atoms/cm^2 and the other describing results on surfaces with greater than 1×10^{15} O atoms/cm^2.

A. Surfaces with Low Oxygen Precoverage

Turnover frequencies for isobutane and *n*-butane formation as a function of O coverage are shown in Fig. 3. Oxygen was a poison to the formation of isobutane. The isobutane rate decreased linearly with O coverage indicating that the effect of oxygen is chiefly geometric rather than electronic in nature. The *n*-butane rate was lower (ca. 5 times lower than the isobutane rate on the initially clean surface) and also decreased linearly with oxygen coverage up to a coverage of 1.5×10^{15} atoms/cm^2.

Turnover frequencies for methane, propane, and ethane formation as a function of oxygen coverage are shown in Fig. 4. Methane and propane turnover frequencies were identical within experimental error in agreement with results on supported Mo catalysts. The methane and propane TOFs were ca. 30 times greater than the ethane TOF on the initially clean Mo(111) surface. In addition, the methane and propane TOFs were ca. 5 times lower than the isobutane TOF on the initially clean surface. This is to be expected because single hydrogenolysis (one C–C bond cleavage) is more facile than double hydrogenolysis (two C–C bond cleavages). The rate of formation of isobutane and all three double-hydrogenolysis products decreased linearly with oxygen coverage. This suggests that the site for the formation of double-hydrogenolysis products is similar to the site active for isobutane production.

Distributions for all hydrogenolysis products as a function of oxygen coverage are shown in Fig. 5. The distribution of single- and double-hydrogenolysis products re-

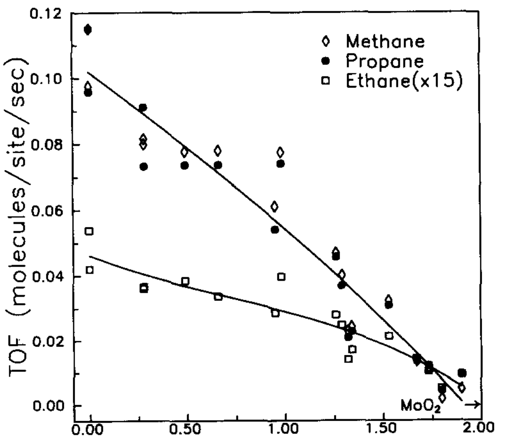

FIG. 4. Turnover frequencies for methane, propane, and ethane formation as a function of oxygen precoverage.

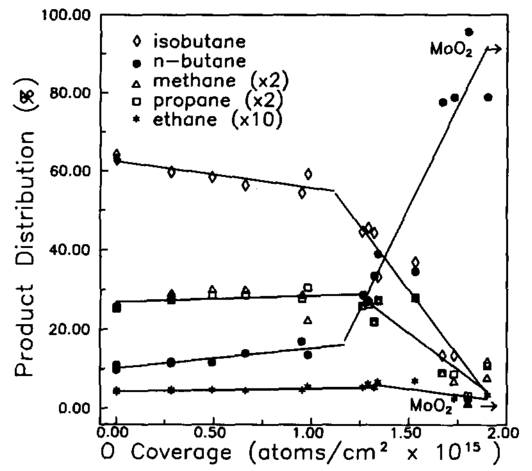

FIG. 5. Product distributions for all hydrogenolysis products as a function of oxygen precoverage.

mained approximately constant at ca. 60% isobutane, 11.5% *n*-butane, 14% propane, 14% methane, and 0.5% ethane up to an oxygen coverage of ca. 1 × 10^{15} atoms/cm^2.

B. Surfaces with High Oxygen Precoverage

As mentioned earlier, results over surfaces with high oxygen precoverage were quite different from those obtained on surfaces with low oxygen precoverages. The most significant difference was in the single hydrogenolysis data. Whereas isobutane formation fell linearly with oxygen coverage and was completely poisoned at oxygen coverages $>1.8 \times 10^{15}$ atoms/cm^2, the *n*-butane rate increased dramatically by a factor of five at oxygen coverages $>1.5 \times 10^{15}$ atoms/cm^2. In addition, the *n*-butane rate in this oxygen coverage regime was essentially the same as that found on MoO_2 (see Fig. 3). The double hydrogenolysis rate behavior was analogous to that of isobutane. The rates fell linearly with increasing oxygen coverage and were completely poisoned at oxygen coverages $>1.8 \times 10^{15}$ atoms/cm^2. At oxygen coverages $>1 \times 10^{15}$ atoms/cm^2, hydrogenolysis product distributions differed significantly from those at low oxygen coverage as shown in Fig. 5. Above 1 × 10^{15} atoms/cm^2, the amount of isobutane and double hydrogenolysis products dropped rapidly with a concomitant rise in the amount of *n*-butane. The product distribution (ca. 100% *n*-butane) at an oxygen coverage of 1.8 × 10^{15} atoms/cm^2 was the same as that found on MoO_2.

Olefins were detected for reaction runs on the MoO_2 surface and the surface with 1.8 × 10^{15} O atoms/cm^2. In reactions over all other surfaces, the olefins present as impurities were hydrogenated immediately, and if any olefins were formed during the reaction they were hydrogenated too quickly to be detected. The hydrogenation activity of the highly oxidized surfaces was low enough that the olefins could build up to a level detectable by GC. 1-Butene and propene were the two olefins of significance that were detected. It was assumed that the olefins would eventually be hydrogenated to *n*-butane and propane. Thus when calculating the TOFs for *n*-butane and propane, 1-butene and propene product accumulations were added in respectively. Each olefin accounted for <10% of its respective paraffin.

Although the hydrogenation rate was lower on the highly oxidized surfaces than on the initially clean Mo(111) surface, the oxidized surfaces were still quite active for olefin hydrogenation. This behavior is consistent with results obtained for olefin hydrogenation on supported Mo catalysts. Although unreduced MoO_3/Al_2O_3 catalysts were inactive, after reduction these catalysts were active for hydrogenation (*33*, *34*). Hydrogenation activity increased with the extent of reduction as one would expect. Similar results were obtained for $Mo(CO)_6/Al_2O_3$ catalysts (*35*, *36*). In addition, bulk MoO_2 has been found to be active for the deuterogenation of ethylene, although the oxide was less active than Mo(0).

Isomerization as well as hydrogenolysis of MCP occurred at 373 K in H_2 over MoO_2 and the surface with 1.8 × 10^{15} O atoms/cm^2. *Cis*- and *trans*-2-butene as well as 1-butene were detected. It was impossible to calculate a meaningful rate of formation for

1-butene over these surfaces because hydrogenation of the resulting olefin and direct hydrogenolysis to *n*-butane could not be distinguished. The *cis*- and *trans*-2-butene peaks partially overlapped the large MCP chromatographic peak in this study; thus it was difficult to measure accurately the amounts formed. However, it is estimated that the total of *cis*- plus *trans*-2-butene amounted to <5% of the *n*-butane production.

The production of isobutene could not be detected due to total overlap with the 1-butene chromatographic peak. Isobutene has been detected in two studies of the isomerization of MCP over MoO_3/Al_2O_3 catalysts (*37, 38*). However, the amount of isobutene formed compared to the *n*-butenes was very small. In other studies of the isomerization of MCP over acidic catalysts only *n*-butenes were formed (*17, 39, 40*). It is therefore unlikely that any significant amount of isobutene was formed on the highly oxidized Mo surfaces in this study. It is certain that no isobutene was formed on the less oxidized surfaces since no olefins were detected.

Two other products, pentane and 1-butyne, were detected in trace amounts on the highly oxidized surfaces. The rates of formation of pentane and 1-butyne were ca. 2.5×10^{-3} molecules/site/s and $<10^{-3}$ molecules/site/s respectively. Pentane probably resulted from the hydrogenation of 2-pentene which is a metathesis product. This is discussed in more detail later. 1-Butyne resulted from the dehydrogenation of 1-butene.

In one experiment, on MoO_2, 750 Torr of Ar was substituted for 750 Torr of H_2. The only products detected were 1-butene and propene. The rate of 1-butene formation was quite low at 0.017 molecules/site/s compared to an average rate of formation of *n*-butane (in the presence of H_2) of 0.21 molecules/site/s over highly oxidized surfaces. As mentioned earlier, it is impossible to calculate the rate of 1-butene formation in the presence of H_2.

DISCUSSION

The results indicate that two mechanisms for MCP hydrogenolysis are operative. One mechanism operates on surfaces with low oxygen precoverage and the other on surfaces with high oxygen precoverage.

A. *Surfaces With Low Oxygen Precoverage*

Isobutane was the major product formed on the initially clean Mo(111) surface and surfaces with oxygen in the chemisorbed phase ($<1 \times 10^{15}$ atoms/cm^2). This is in agreement with a majority of studies on metal films and supported metal catalysts reported in the literature. The rate of isobutane formation fell linearly with oxygen coverage and the selectivity to isobutane remained constant until oxide began to form. The double hydrogenolysis production rate as a function of oxygen coverage was similar to that for isobutane. The rate of double hydrogenolysis decreased with increasing oxygen precoverage and the isobutane and double hydrogenolysis rates approached zero at exactly the same oxygen coverage. In addition, the double hydrogenolysis product distribution was constant below 1.5×10^{15} O atoms/cm^2. The fact that product selectivity was constant for oxygen coverages between 0 and 1×10^{15} atoms/cm^2 while activity fell by a factor of two over this same range of coverages suggests that a single type of active site is responsible for all products and that this site is poisoned by oxygen. In particular, formation of *n*-butane over surfaces with low oxygen coverage by the acid-catalyzed mechanism operative at high oxygen coverages (see below) is inconsistent with (1) the observed poisoning by chemisorbed oxygen and (2) the formation of ethane double hydrogenolysis product. Poisoning of *n*-butane formation may not be so evident from the data in Fig. 3 but is clearly demonstrated by the constant product selectivity shown in Fig. 5 for coverages $<1 \times 10^{15}$ O atoms/cm^2.

These results agree with previous results for the hydrogenolysis of cyclopropane on an initially clean Mo(100) surface and surfaces chemically modified with 1 ML (monolayer) of oxygen and 1 ML of carbon (*27*). The active sites for this reaction were assigned to be fourfold hollows of metallic character present in high concentration on the initially clean surface and as defects on the chemically modified surfaces. Interestingly, the activation energy and product distribution were the same on all three surfaces. The activity of the clean surface, however, was higher than that of the C- and O-modified surfaces. Thus, our results, which show a constant product distribution below 1 × 10^{15} O atoms/cm^2 and a decrease in activity with oxygen precoverage, are consistent with an active site of metallic character.

It is likely that double hydrogenolysis and single hydrogenolysis on metallic sites go through the same intermediate. Two intermediates have been proposed to account for isobutane and *n*-butane formation on metal surfaces and are shown below (*6*).

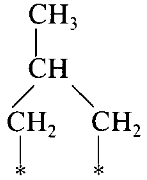

(1)

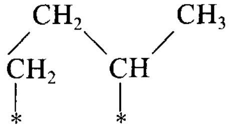

(2)

Whether in the present case these two intermediates are bound to two Mo atoms, as shown, or to one Mo atom (metallacyclobutane) is not known.

Support for these intermediates comes from double hydrogenolysis product distributions. Double hydrogenolysis of (1) would yield only methane and propane in equal amounts. Double hydrogenolysis of (2) would yield either methane plus propane in equal amounts or two equivalents of ethane. Results obtained show that equal amounts of methane and propane were formed on metallic Mo. Furthermore, ethane was formed in smaller amounts than methane and propane. This is to be expected if (1) is the preferred surface intermediate.

B. Surfaces With High Oxygen Precoverage

n-Butane was a minor hydrogenolysis product on metallic Mo. Once oxide formation began, however, the selectivity to *n*-butane increased. At O coverages >1.5 × 10^{15} atoms/cm^2, the selectivity to *n*-butane approached 100% and the TOF increased by a factor of five. The selectivity change is consistent with a shift from a metallic mechanism to one involving ionic Mo. This mechanistic change occurs abruptly, just as the metal-to-oxide transition occurs abruptly for Mo as determined by XPS (*20, 21*). One would expect the mechanistic change and metal-to-oxide transition to occur in the same oxygen coverage range, but the fact that they occur at almost exactly the same coverage is remarkable. Since oxide must be present for the mechanistic change, this indicates that a Mo cation, probably with an oxidation state of +4, is associated with the active site. Mo cations are Lewis acids and hence the likely site for MCP adsorption since the cyclopropane ring has olefinic character making it a Lewis base. However, this does not explain the observed product selectivity.

There are two possible mechanisms which depend on the presence of coordinatively unsaturated (cus) Mo ions that are consistent with the observed product selectivity. Both mechanisms involve acidic attack on the cyclopropane ring, but they differ in the nature of the acid responsible. The first possibility involves the formation of metallacyclobutane on the surface.

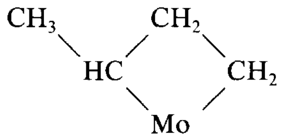

Metallacyclobutane is formed by electrophilic insertion of the cus Mo cation into the cyclopropane ring. As mentioned earlier, the C–C bonds adjacent to the point of substitution have the highest electron density; thus, the cation would preferentially insert into the C_1–C_2 or C_1–C_3 bonds. We view this as a Lewis acid attack on the cyclopropane ring. Direct hydrogenation of the metallacyclobutane followed by desorption yields *n*-butane.

It is also possible for *n*-butane to be formed by isomerization to one of the *n*-butenes followed by hydrogenation. If isomerization is required in the formation of *n*-butane, one would expect to observe formation of 1-butene in Ar at a rate approximately equal to the 1-butene + *n*-butane rate in H_2. Although, 1-butene formation was, indeed, observed over oxidized surfaces in either H_2 or Ar, the rate of formation in Ar was one order of magnitude lower than that of *n*-butane in H_2. Since there was no deactivation or carbon deposition in Ar neither of these effects can account for the significantly lower isomerization rate. Another possibility which cannot be ruled out is that H_2 activates the surface for isomerization. However, without a knowledge of the 1-butene formation rate in the presence of H_2, one cannot be more definitive.

Further support for the metallacyclobutane intermediate is the presence of pentane product on the heavily oxidized surfaces. Metallacyclobutanes are known to be intermediates in olefin metathesis reactions. In metathesis the metallacyclobutane decomposes to form a surface carbene. The carbene can react with 1-butene to form 2-pentene which is hydrogenated to produce pentane:

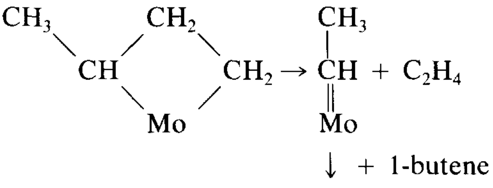

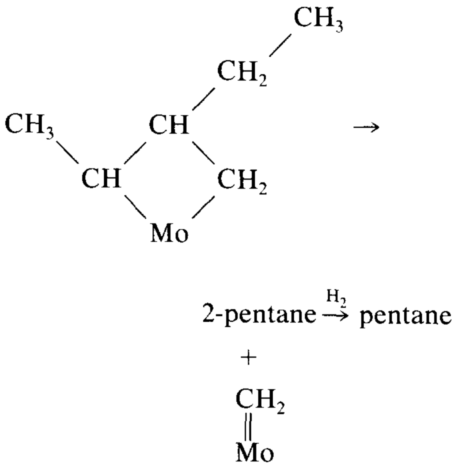

Trace quantities of C_2H_4/C_2H_6, the other metathesis product, are also observed on the highly oxidized surfaces. Evidence for stable carbene complexes on Mo catalysts has been reported previously using IR spectroscopy (*41*).

The second mechanism involves formation of a secondary carbenium ion by a Brønsted acid mechanism. Protonic ring-opening mechanisms have been proposed to account for the results of isomerization of alkylcyclopropanes over a SiO_2–Al_2O_3 (*17, 40*) catalyst as well as the hydrogenolysis of 1,1-dimethylcyclopropane over an acidic Ni/Al_2O_3 catalyst (*9*). It was suggested that the protons are formed by heterolytic dissociation of H_2 on Lewis acid and base sites of the catalyst. For the present catalyst system, Mo cations are Lewis acids, oxygen anions are Lewis bases, and protons would be derived from hydroxyl groups formed on the surface. It has also been suggested that protons may be provided by carbonaceous residue held on Lewis acid sites (*16, 40*), but this possibility appears unlikely in the present case due to the absence of any carbon residue on the oxide surface following reaction (see Fig. 1). Proton addition to C_2 or C_3 of MCP would induce C_1–C_2 or C_1–C_3 bond cleavage resulting in a secondary carbenium ion intermediate. The intermediate can then react by two different pathways. Addition of a hydride ion would result in *n*-

butane. Loss of a proton would result in 1-butene, *cis*-2-butene, or *trans*-2-butene. This mechanism would also account for the absence of isobutene and isobutane on the oxidized surfaces. Isobutene(ane) would be derived from a primary carbenium ion which is unstable.

Between these two mechanisms we favor the first. From our previous work there is strong spectroscopic evidence that Mo cations are present on the oxidized surface (*21*) and strong chemical evidence that these cations behave as hard Lewis acids (*42*). In addition, Hall and co-workers (*37*) have shown convincingly that a Brønsted acid mechanism is not operative for cyclopropane (CP) isomerization over molybdena/alumina based on (1) the observation that Brønsted sites disappear with catalyst reduction while the activity for CP conversion increases; (2) the observation that CP activity decreases when Brønsted sites are introduced by addition of water to the catalyst; and (3) the detection of small amounts of isobutene from MCP isomerization which is not an acid-catalyzed product. On the other hand it should be noted that the evidence pertaining to MCP conversion reported in Ref. (*37*) is less decisive. Whereas the activity for CP conversion increased with catalyst reduction, the opposite trend was observed for MCP. The effect of added water on MCP activity was not reported (*37*). Finally, from the results reported here where isobutane formation was detected only on the metallic molybdenum sites one may wonder whether isobutene formation occurred on a small number of such sites present on the catalysts of Ref. (*37*). In the absence of definitive evidence to the contrary it is not possible at present to rule out a Brønsted acid mechanism for MCP hydrogenolysis over the Mo(111) surfaces with high oxygen precoverage.

Results from this study offer insight into questions concerning hydrogenolysis and isomerization of alkanes and cycloalkanes over supported Mo catalysts. Burwell and Chung studied the hydrogenolysis of MCP over highly reduced MoO_3/Al_2O_3 and $Mo(CO)_6/Al_2O_3$ catalysts (*15, 16*). These catalysts were pretreated such that the molybdenum was in the metallic state. *n*-Butane instead of isobutane, however, was the major single hydrogenolysis product obtained. The alumina was eliminated as a source of extra *n*-butane because the conversion was too small. In addition, the MoO_3 and $Mo(CO)_6$ catalysts were prepared under very different conditions so it is improbable that the same active sites could be formed on the alumina. The other two explanations put forth by the authors were that (1) excess *n*-butane was formed on Mo or (2) *n*-butane may be formed at acidic sites located at the interface between Mo and Al_2O_3. Our results support the latter suggestion because Mo metal is similar to most metals in that isobutane is the major product.

Holl *et al.* studied the isomerization and hydrogenolysis of various alkanes over Mo film, Mo powder, and highly reduced MoO_3/Al_2O_3 catalysts (*43, 44*). The MoO_3/Al_2O_3 catalyst was reduced under similar conditions to those of Burwell and co-workers (*45*). The Mo powder was reduced in H_2 for 15 h. The Mo film was the only catalyst with high activity for hydrogenolysis. The other two catalysts had lower activity and high selectivity (>90%) for isomerization. All three catalysts were assumed to contain metallic Mo. Holl *et al.* suggested that the hydrogenolysis activity of the Mo film could be due to traces of impurities around the Mo aggregates or that the glass support could have an effect on the reaction. Our results, as well as those of Burwell and co-workers (*15, 16, 46–48*), show that Mo metal is very active for hydrogenolysis and that Holl's explanation is not satisfactory. In addition, it is hard to understand why the Mo powder and highly reduced MoO_3/Al_2O_3 catalysts would have such low activity for hydrogenolysis and high selectivity for isomerization if the catalysts contained Mo metal. We agree with Burwell and co-workers (*16, 49*) and

Hall and co-workers (*50*) and conclude that these catalysts could not have been "clean." They must have been poisoned by oxygen or other contaminants.

CONCLUSIONS

Two mechanisms are operative in the reaction of MCP with H_2 over the initially clean Mo surface and surfaces with varying amounts of oxygen. MCP reacted with H_2 over initially clean Mo to give isobutane as a major single hydrogenolysis product and *n*-butane as a minor one. In addition, equal amounts of methane and propane, as well as a small amount of ethane, were formed as double hydrogenolysis products. Isobutane, *n*-butane, methane, propane, and ethane were formed on metallic Mo. Oxygen acted as a poison for these products. It should be noted, as a consequence of this result, that acid sites are not required to form *n*-butane from MCP. This fact has not been recognized in the past. *n*-Butane, on the other hand, was formed preferentially on the oxidized Mo surface. The increase in *n*-butane TOF was coincident with oxide formation on Mo as determined by XPS. The product distribution on the oxidized surface can be adequately explained by a Lewis or Brønsted acid mechanism.

ACKNOWLEDGMENTS

The authors are grateful for helpful discussions with Professors Robert L. Burwell, Jr. and Herman Pines. This material is based upon work supported by the National Science Foundation under Award No. CHE-8821781.

REFERENCES

1. Hoffman, R., *Tetrahedron Lett.*, 2907 (1970).
2. Irwin, W. J., and McQuillin, F. J., *Tetrahedron Lett.*, 2195 (1968).
3. Bond, G. C., and Newham, J., *J. Trans. Faraday Soc.* **56,** 1501 (1960).
4. Maire, G., Plouidy, G., Prudhomme, J. C., and Gault, F. G., *J. Catal.* **4,** 556 (1965).
5. Chevreau, T., and Gault, F. G., *J. Catal.* **50,** 124 (1977).
6. Anderson, J. R., and Avery, N. R., *J. Catal.* **8,** 48 (1967).
7. Newham, J., *Chem. Rev.* **63,** 123 (1963), and references therein.
8. Wong, S. S., Otero-Schipper, P. H., Wachter, W. A., Inoue, Y., Kobayashi, M., Butt, J. B., Burwell, R. L., Jr., and Cohen, J. B., *J. Catal.* **64,** 84 (1980).
9. Pines, H. and Nogueira, L., *J. Catal.* **27,** 89 (1972).
10. Schlatter, J. C., and Boudart, M., *J. Catal.* **25,** 93 (1972).
11. Otero-Schipper, P. H., Wachter, W. A., Butt, J. B., Burwell, R. L., Jr., and Cohen, J. B., *J. Catal.* **50,** 494 (1977).
12. Otero-Schipper, P. H., Wachter, W. A., Butt, J. B., Burwell, R. L., Jr., and Cohen, J. B., *J. Catal.* **53,** 414 (1978).
13. Notheisz, F., Palinko, I., and Bartok, M., *Catal. Lett.* **5,** 229 (1990).
14. Engstrom, J. R., Goodman, D. W., and Weinberg, W. H., *J. Phys. Chem.* **94,** 396 (1990).
15. Burwell, R. L., Jr., and Chung, J., *React. Kinet. Catal. Lett.* **35,** 381 (1987).
16. Chung, J., and Burwell, R. L., Jr., *J. Catal.* **116,** 519 (1989).
17. Hightower, J. W., and Hall, W. K., *J. Am. Chem. Soc.* **90,** 851 (1968).
18. Bartok, M., Palinko, I., and Molnar, A., *J. Chem. Soc., Chem. Commun.*, 953 (1987).
19. Palinko, I., Molnar, A., Kiss, J. T., and Bartok, M., *J. Catal.* **121,** 396 (1990).
20. Henry, R. M., Fryberger, T. A. B., and Stair, P. C., *J. Vac. Sci. Technol.* **20,** 818 (1982).
21. Fryberger, T. B., and Stair, P. C., *Chem. Phys. Letters* **93,** 151 (1982).
22. Grant, J. L., Fryberger, T. B., and Stair, P. C., *Surf. Sci.* **159,** 333 (1985).
23. Henry, R. M., Walker, B. W., and Stair, P. C., *Surf. Sci.* **155,** 732 (1985).
24. Kennett, H. M., and Lee, A. E., *Surf. Sci.* **48,** 591 (1975).
25. Kennett, H. M., and Lee, A. E., *Surf. Sci.* **48,** 606 (1975).
26. Zhang, C., Van Hove, M. A., and Somorjai, G. A., *Surf. Sci.* **149,** 326 (1985).
27. Kellogg, D. S., Touvelle, M. S., and Stair, P. C., *J. Catal.* **120,** 192 (1989).
28. Zhang, C., Gellman, A. J., Farias, M. H., and Somorjai, G. A., *Mat. Res. Bull.* **20,** 1129 (1985).
29. Ferrante, J., and Barton, G. C., NASA TN D-4735.
30. Walker, B. W., and Stair, P. C., *Surf. Sci.* **103,** 315 (1981).
31. Smudde, G., and Stair, P. C., in press.
32. Felter, T. E., and Estrup, P. J., *Surf. Sci.* **54,** 197 (1976).
33. Lombardo, E. A., Lo Jacono, M., and Hall, W. K., *J. Catal.* **64,** 150 (1980).

34. Lombardo, E. A., Houalla, M., and Hall, W. K., *J. Catal.* **51,** 256 (1978).

35. Bowman, R. G., and Burwell, R. L., Jr., *J. Catal.* **88,** 388 (1984).

36. Nazario, P., and Brenner, A., *in* "Proceedings, 9th International Congress on Catalysis, Calgary, 1988." (M. J. Phillips and M. Ternan, Eds.), p. 1020. Chem. Institute of Canada, Ottawa, 1988.

37. Hall, W. K., Schneider, R. L., and Goldwasser, J., *in* "Proceedings, 8th International Congress on Catalysis, Berlin, 1984," pp. IV–273. Dechema, Frankfurt-am-Main, 1984.

38. Otremba, M., and Taniewski, M., *J. Catal.* **31,** 419 (1973).

39. Lombardo, E. A., Lo Jacono, M., and Hall, W. K., *J. Catal.* **51,** 243 (1978).

40. Gerberich, H. R., Hightower, J. W., Hall, W. K., *J. Catal.* **8,** 391 (1967).

41. Vikulov, K. A., Elev, I. V., Shelimov, B. N., and Kazansky, V. B., *Catal. Lett.* **2,** 121 (1989).

42. Deffeyes, J. E., Smith, A. H., and Stair, P. C., *Surf. Sci.* **163,** 79 (1985).

43. Holl, Y., Garin, F., Maire, G., Muller, A., Engelhard, P. A., and Grosmangin, J., *J. Catal.* **104,** 211 (1987).

44. Holl, Y., Garin, F., Maire, G., Muller, A., Engelhard, P. A., and Grosmangin, J., *J. Catal.* **104,** 225 (1987).

45. Chung, J., Zhang, J. P., and Burwell, R. L., Jr., *J. Catal.* **116,** 506 (1989).

46. Nakamura, R., Bowman, R. G., and Burwell, R. L., Jr., *J. Am. Chem. Soc.* **103,** 673 (1981).

47. Nakamura, R., Pioch, D., Bowman, R. G., and Burwell, R. L., Jr., *J. Catal.* **93,** 388 (1985).

48. Nakamura, R., and Burwell, R. L., Jr., *J. Catal.* **93,** 399 (1985).

49. Burwell, R. L., Jr., *J. Catal.* **113,** 567 (1988).

50. Redey, A., Goldwasser, J., and Hall, W. K., *J. Catal.* **113,** 82 (1988).